GSA Data Repository Item 2017262
Duan, L., Meng, Q.-R., Christie-Blick, N., and Wu, G.-L., 2017, New insights on the Triassic tectonic development of South China from the detrital zircon provenance of Nanpanjiang turbidites: GSA Bulletin, doi:10.1130/B31630.1.

DATA REPOSITORY

Table DR1. U-Pb ages and Hf isotopes

Table DR2. K-S test result

Analytical Methods

Zircon crystals were extracted from samples by standard density and magnetic separation techniques and then purified by hand picking >1000 zircon grains under a binocular microscope. Representative zircon grains were handpicked and mounted in epoxy resin discs, then polished and coated with gold. All analyzed zircon grains were documented using cathodoluminescence (CL) images for internal morphology prior to analysis, using a Mono CL3+ (Gatan, USA) attached to a scanning electron microscope (Quanta 400 FEG). Before analysis, the surface was cleaned using dilute HNO_3 (3%, v/v) and pure alcohol to remove any lead contamination. CL imaging, U–Pb dating and Hf-isotope analysis were carried out in the State Key Laboratory of Continental Dynamics, Northwest University, Xi'an.

U-Pb Dating

Approximately 100 randomly selected detrital zircon grains were analyzed from each sample. U-Pb geochronology of zircon grains was conducted by laser ablation–inductively coupled plasma–mass spectrometry (LA-ICP-MS). The ICP-MS used is a Varian 820-MS (Varian, Inc., USA), and the analyses involve ablation of zircon with the GeoLas 2005 laser-ablation system (MicroLas^{TM} Beam Delivery Systems, Lambda Physik AG, Germany) (operating at a wavelength of 193 nm), and using a spot diameter of 44 μm. In this technique, zircons are sampled using a focused UV laser, and the ablated microparticulate material is transferred in a continuous flow of helium to an ICP-MS for isotopic quantification. The laser frequency used was 10 Hz. Raw count rates were measured for ^{29}Si, ^{204}Pb, ^{206}Pb, ^{207}Pb, ^{208}Pb, ^{232}Th and ^{238}U. U, Th and Pb concentrations were calibrated by using ^{29}Si as an internal standard and NIST 610 as the reference standard. ^{207}Pb/^{206}Pb, ^{206}Pb/^{238}U, ^{207}Pb/^{235}U and ^{208}Pb/^{232}Th ratios were then calculated using the GLITTER 4.0 program (Macquarie University). Finally they were corrected for both instrumental mass bias and depth-dependent elemental and isotopic fractionation using Harvard zircon 91500 as external standard. The detailed analytical technique is summarized in Yuan et al. (2004). Age calculations were made using ISOPLOT 3.0 (Ludwig, 2003) for results with 1σ errors.

Lu-Hf Isotope Analysis

In situ zircon Hf isotopic analyses were conducted using a Nu Plasma HR MC-ICP-MS (Nu Instruments Ltd., UK), coupled to a GeoLas 2005 excimer ArF laser-ablation system. In this study, Hf isotopes and trace element compositions of zircon were obtained simultaneously and from the same spots with the determination of U–Pb age, by combining excimer laser ablation quadruple and multiple collector ICP-MS (Yuan et al. 2008). The energy density applied was 15–20 J/cm^2 and spot sizes of 44μm, with a laser repetition rate of 10 Hz, were used. The detailed analytical technique is described in Yuan et al. (2008). Raw count rates for ^{172}Yb, ^{173}Yb, ^{175}Lu, ^{176}(Hf+Yb+Lu), ^{177}Hf, ^{178}Hf, ^{179}Hf, ^{180}Hf and ^{182}W were collected. Interference of ^{176}Lu on ^{176}Hf was corrected by measuring the intensity of the interference-free ^{175}Lu isotope and using the recommended ^{176}Lu/^{175}Lu ratio of 0.02655 (Chu et al., 2002). A ^{176}Yb/^{172}Yb of 0.5887 and mean β_{Yb} obtained during Hf analysis were applied for the interference correction of ^{176}Yb on ^{176}Hf (Iizuka and Hirata, 2005). During analyses, Harvard zircon 91500 was used as the reference standard, the obtained ^{176}Hf/^{177}Hf ratio was 0.282304 ± 14 (2σ, n = 19), similar to the recommended ^{176}Hf/^{177}Hf ratio of 0.282306 ± 10 measured using the solution method (Woodhead et al., 2004). The measured ^{176}Lu/^{177}Hf ratios and the ^{176}Lu decay constant of 1.867 × 10^{-11} yr^{-1} reported by Soderlund et al. (2004) were adopted to calculate initial ^{176}Hf/^{177}Hf ratios. The chondritic values of ^{176}Hf/^{177}Hf and ^{176}Lu/^{177}Hf reported by Blichert-Toft and Albarède (1997) were used for the calculation of ε_{Hf} values. Single-stage model ages (T_{DM1}) were calculated relative to the depleted mantle with a present-day (^{176}Lu/^{177}Hf)$_{DM}$ = 0.0384 and (^{176}Hf/^{177}Hf)$_{DM}$ = 0.28325 (Griffin et al., 2000); two-stage continental model age (T_{DM}^{C}) was also calculated by projecting the initial ^{176}Hf/^{177}Hf of zircon back to the depleted mantle growth curve using ^{176}Lu/^{177}Hf = 0.015 for the average continental crust (Griffin et al., 2000; Yang et al., 2006). The notations of $\varepsilon_{Hf(t)}$, $f_{Lu/Hf}$, T_{DM}^{1} and T_{DM}^{C} are defined as same as those in Yang et al. (2006).

Comparisons of zircon U–Pb age-distribution curves were made by cumulative probability plots and Kolmogorov-Smirnov (K-S) P value determinations using Microsoft Excel macros developed by Gehrels (2011). The fundamental criterion of similarity is the P value, which is the probability that two samples are not statistically different. All probabilities (*p* values) > 0.05 indicate >95% confidence that the pair of samples are not statistically different (Gehrels, 2011).

REFERENCES CITED

Blichert-Toft, J., and Albarède, F., 1997, The Lu–Hf isotope geochemistry of chondrites and the evolution of the mantle–crust system: Earth and Planetary Science Letters, v. 148, p. 243–258, https://doi.org/10.1016/S0012-821X(97)00040-X.

Chu, N.C., Taylor, R.N., Chavagnac, V., Nesbitt, R.W., Boella, R.M., Milton, J.A., German, C.R., Bayon, G., and Burton, K., 2002, Hf isotope ratio analysis using multi-collector inductively coupled plasma mass spectrometry: an evaluation of isobaric interference corrections: Journal of Analytical Atomic Spectrometry, v. 17, p. 1567–1574, https://doi.org/10.1039/b206707b.

Gehrels, G., 2011, Detrital zircon U-Pb geochronology: Current methods and new opportunities, *in* Busby, C., and Azor-Pérez, A., eds., Recent Advances in Tectonics of Sedimentary Basins: Chichester, UK, John Wiley & Sons, 664 p., https://doi.org/10.1002/9781444347166.ch2.

Griffin, W.L., Pearson, N.J., Belousova, E., Jackson, S.E., Achterbergh, E.V., O'Reilly, S.Y., and Shee, S.R., 2000, The Hf isotope composition of cratonic mantle: LAM-MC-ICPMS

analysis of zircon megacrysts in kimberlites: Geochimica et Cosmochimica Acta, v. 64, p. 133–147, https://doi.org/10.1016/S0016-7037(99)00343-9.
Iizuka, T., and Hirata, T., 2005, Improvements of precision and accuracy in in-situ Hf isotope microanalysis of zircon using the laser ablation-MC-ICPMS technique: Chemical Geology, v. 220, p. 121–137, https://doi.org/10.1016/j.chemgeo.2005.03.010.
Ludwig, K.R., 2003, ISOPLOT 3: a geochronological toolkit for Microsoft excel: Berkeley Geochronology Centre Special Publication 4, 74 p.
Liu, B., and Xu, X., 1994, Atlas of Lithofacies and Paleogeography of South China: Beijing, Science Press, 188 p.
Ma, Y., Chen, H., and Wang, G., 2009, Atlas of Tectono-sequence Lithofacies and Paleogeography of South China: Beijing, Science Press, 301 p.
Soderlund, U., Patchett, P.J., Vervoort, J.D. and Isachsen, C.E., 2004, The ^{176}Lu decay constant determined by Lu–Hf and U–Pb isotope systematics of Precambrian mafic intrusions: Earth and Planetary Science Letters, v. 219, p. 311–324, https://doi.org/10.1016/S0012-821X(04)00012-3.
Woodhead, J., Hergt, J., Shelley, M., Eggins, S., and Kemp, R., 2004, Zircon Hf-isotope analysis with an excimer laser, depth profiling, ablation of complex geometries, and concomitant age estimation: Chemical Geology, v. 209, p. 121–135, https://doi.org/10.1016/j.chemgeo.2004.04.026.
Yang, J.H., Wu, F.Y., Chung, S.L., Wilde, S.A., and Chu, M.F., 2006, Constraints on the timing of uplift of the Yanshan Fold and Thrust Belt, North China: Earth and Planetary Science Letters, v. 246, p. 336–352, https://doi.org/10.1016/j.epsl.2006.04.029.
Yuan, H.L., Gao, S., Dai, M.N., Zong, C.L., Günther, D., Fontaine, G.H., Liu, X.M., and Diwu, C.R., 2008, Simultaneous determinations of U–Pb age, Hf isotopes and trace element compositions of zircon by excimer laser ablation quadrupole and multiple collector ICP-MS: Chemical Geology, v. 247, p. 100–118, https://doi.org/10.1016/j.chemgeo.2007.10.003.
Yuan, H.L., Gao, S., Liu, X.M., Li, H.M., Günther, D., and Wu, F.Y., 2004, Accurate U–Pb age and trace element determinations of zircon by laser ablation-inductively coupled plasma mass spectrometry: Geoanalytical and Geostandard Research, v. 28, p. 353–370, https://doi.org/10.1111/j.1751-908X.2004.tb00755.x.

Fig. DR1. Field picture of Middle Triassic fluvial floodplain deposits outcrop in Heshan County, Guangxi Province (N 23º44’39.7”, E 108º55’12.0”). Circled hammer for scale.

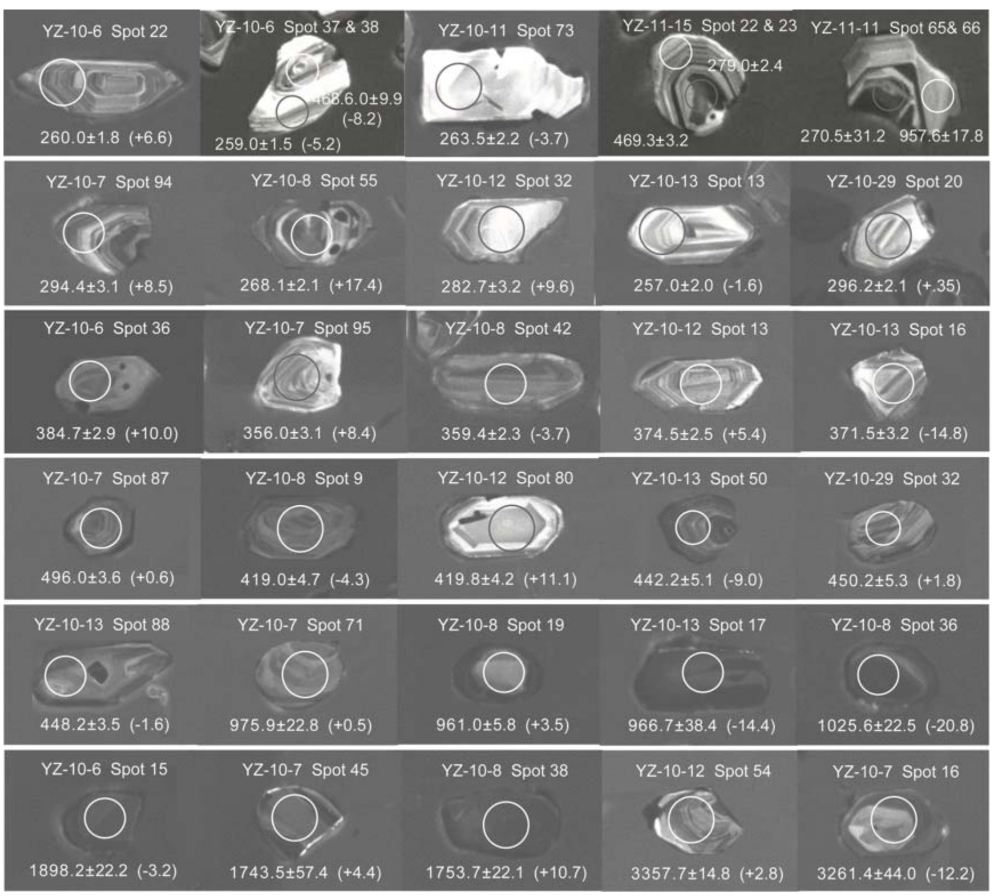

Fig. DR2. Photomicrographs of representative detrital zircon grains in distinct age populations. Results of U–Pb ages and $\varepsilon_{Hf(t)}$ values (within parentheses) are marked with circles, representing the analytical spots. Diameter of all analytical spots is 44 μm.

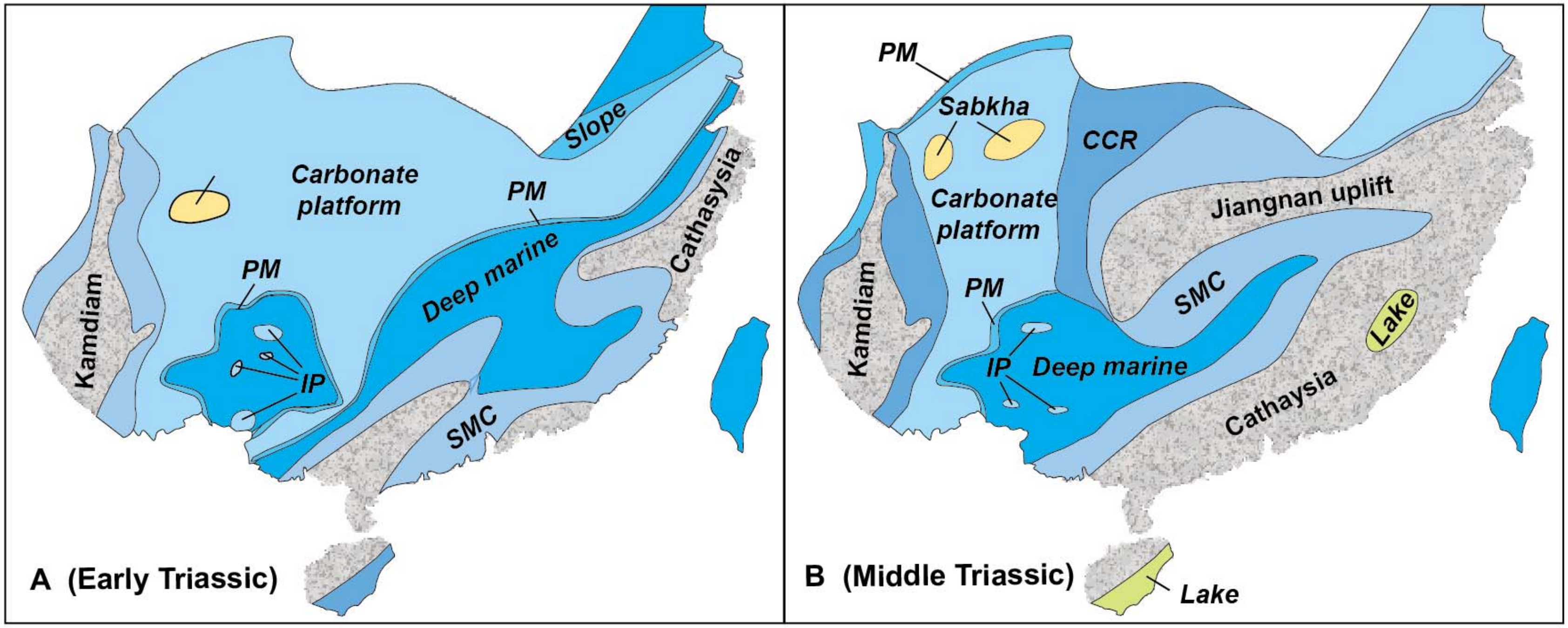

Fig. DR3. Early and Middle Triassic paleogeographic maps of South China (modified after Liu and Xu, 1994; Ma et al., 2009). CCR—carbonate-clastic ramp; IP—isolated platform; PMR—platform margin reef; SCM—shallow marine clastic.

Table DR2. K-S test result

K-S P-values using error in the CDF

	YZ-10-29	YZ-10-6	YZ-10-7	YZ-10-8	YZ-10-12	YZ-10-13	YZ-11-11	YZ-11-15
YZ-10-29		0.002	**0.566**	**0.465**	**0.166**	0.000	0.000	0.000
YZ-10-6	0.002		0.046	0.016	**0.117**	**0.569**	**0.332**	**0.091**
YZ-10-7	**0.566**	0.046		**0.995**	**0.924**	0.015	0.016	0.000
YZ-10-8	**0.465**	0.016	**0.995**		**0.990**	0.006	0.001	0.000
YZ-10-12	**0.166**	**0.117**	**0.924**	**0.990**		0.044	0.012	0.001
YZ-10-13	0.000	**0.569**	0.015	0.006	0.044		**0.091**	**0.496**
YZ-11-11	0.000	**0.332**	0.016	0.001	0.012	**0.091**		**0.194**
YZ-11-15	0.000	**0.091**	0.000	0.000	0.001	**0.496**	**0.194**	

D-values using error in the CDF

	YZ-10-29	YZ-10-6	YZ-10-7	YZ-10-8	YZ-10-12	YZ-10-13	YZ-11-11	YZ-11-15
YZ-10-29		0.274	0.117	0.127	0.167	0.314	0.338	0.394
YZ-10-6	0.274		0.205	0.233	0.179	0.119	0.142	0.185
YZ-10-7	0.117	0.205		0.063	0.082	0.236	0.233	0.312
YZ-10-8	0.127	0.233	0.063		0.066	0.259	0.289	0.355
YZ-10-12	0.167	0.179	0.082	0.066		0.211	0.241	0.301
YZ-10-13	0.314	0.119	0.236	0.259	0.211		0.190	0.126
YZ-11-11	0.338	0.142	0.233	0.289	0.241	0.190		0.161
YZ-11-15	0.394	0.185	0.312	0.355	0.301	0.126	0.161	

K-S P-values for no error

	YZ-10-29	YZ-10-6	YZ-10-7	YZ-10-8	YZ-10-12	YZ-10-13	YZ-11-11	YZ-11-15
YZ-10-29		0.001	0.539	0.354	0.167	0.000	0.000	0.000
YZ-10-6	0.001		0.036	0.009	0.061	0.361	0.150	0.070
YZ-10-7	0.539	0.036		0.988	0.914	0.008	0.012	0.000
YZ-10-8	0.354	0.009	0.988		0.972	0.004	0.001	0.000
YZ-10-12	0.167	0.061	0.914	0.972		0.032	0.008	0.000
YZ-10-13	0.000	0.361	0.008	0.004	0.032		0.065	0.442
YZ-11-11	0.000	0.150	0.012	0.001	0.008	0.065		0.098
YZ-11-15	0.000	0.070	0.000	0.000	0.000	0.442	0.098	

D-values for no error

	YZ-10-29	YZ-10-6	YZ-10-7	YZ-10-8	YZ-10-12	YZ-10-13	YZ-11-11	YZ-11-15
YZ-10-29		0.284	0.119	0.139	0.167	0.325	0.357	0.415
YZ-10-6	0.284		0.211	0.247	0.198	0.140	0.171	0.193
YZ-10-7	0.119	0.211		0.067	0.084	0.252	0.240	0.319
YZ-10-8	0.139	0.247	0.067		0.073	0.268	0.299	0.378
YZ-10-12	0.167	0.198	0.084	0.073		0.220	0.250	0.329
YZ-10-13	0.325	0.140	0.252	0.268	0.220		0.200	0.131
YZ-11-11	0.357	0.171	0.240	0.299	0.250	0.200		0.184
YZ-11-15	0.415	0.193	0.319	0.378	0.329	0.131	0.184	

Average K-S P-values using Monte-Carlo

	YZ-10-29	YZ-10-6	YZ-10-7	YZ-10-8	YZ-10-12	YZ-10-13	YZ-11-11	YZ-11-15
YZ-10-29		0.001	0.492	0.381	0.168	0.000	0.000	0.000
YZ-10-6	0.001		**0.041**	0.010	**0.073**	0.349	0.189	**0.053**
YZ-10-7	0.492	**0.041**		0.975	0.897	0.010	0.009	0.000
YZ-10-8	0.381	0.010	0.975		0.957	0.003	0.001	0.000
YZ-10-12	0.168	**0.073**	0.897	0.957		0.029	0.009	0.000
YZ-10-13	0.000	0.349	0.010	0.003	0.029		**0.067**	0.474
YZ-11-11	0.000	0.189	0.009	0.001	0.009	**0.067**		0.122
YZ-11-15	0.000	**0.053**	0.000	0.000	0.000	0.474	0.122	

Two std devs. of P-values using Monte-Carlo

	YZ-10-29	YZ-10-6	YZ-10-7	YZ-10-8	YZ-10-12	YZ-10-13	YZ-11-11	YZ-11-15
YZ-10-29		0.001	0.108	0.121	0.006	0.000	0.000	0.000
YZ-10-6	0.001		**0.016**	0.007	**0.041**	0.107	0.105	**0.026**
YZ-10-7	0.108	**0.016**		0.050	0.084	0.008	0.006	0.000
YZ-10-8	0.121	0.007	0.050		0.053	0.002	0.001	0.000
YZ-10-12	0.006	**0.041**	0.084	0.053		0.017	0.006	0.000
YZ-10-13	0.000	0.107	0.008	0.002	0.017		**0.032**	0.110
YZ-11-11	0.000	0.105	0.006	0.001	0.006	**0.032**		0.065
YZ-11-15	0.000	**0.026**	0.000	0.000	0.000	0.110	0.065	